

# Interaction between rare earth silicate glasses (RE=Y, La, Nd, Dy) and silicon carbide substrates

J. Marchi\*, J.C. Bressiani, A.H.A. Bressiani

IPEN Instituto de Pesquisas Energéticas e Nucleares, CCTM Centro de Ciência e Tecnologia de Materiais, Cidade Universitária, Travessa R 400, 05508-900 São Paulo, Brazil

## Abstract

In this work, the interaction behavior between rare earth silicate glass and green body silicon carbide was studied. Glass compositions prepared were 60%SiO<sub>2</sub>–20%Al<sub>2</sub>O<sub>3</sub>–20%RE<sub>2</sub>O<sub>3</sub> (mol%), RE=Y, La, Nd and Dy. β-SiC powder was consolidated through cold isostatic pressing to obtain specimens of approximately 55% of the theoretical density. Glass/SiC pairs were treated in a graphite resistance furnace at 1500 °C for 1 h, under argon atmosphere. The cross-section of specimens was observed on scanning electron microscope. The distribution profile of rare earth element through the glass/SiC interaction zone was analyzed by energy dispersive spectroscopy.

© 2002 Elsevier Science B.V. All rights reserved.

*Keywords:* Surfaces and interfaces; Powder metallurgy; Scanning electron microscopy; X-ray diffraction

## 1. Introduction

Rare earth glasses are commonly applied in lasers, sensors, radiation shield glasses and in many other uses due to their unique optical and magnetic behavior [1]. Rare earth aluminosilicate-based glasses have been successfully used as *in vivo* radiation delivery vehicles. In this type of application, glasses should be biocompatible, nontoxic and chemically insoluble, to prevent radioactivity leakage within the *in vivo* treatment site [2]. Additionally, yttrium glasses, in the form of microspheres or seeds, have received great attention in the treatment of primary hepatocellular carcinoma, irradiation of diseased synovial membrane for the treatment of rheumatoid arthritis, and treatment of prostate tumors [2].

Rare earth aluminosilicate-based glasses have also been found useful to promote liquid-phase sintering of silicon carbide-based ceramics [3–5]. In these glasses, SiO<sub>4</sub> tetrahedrons are bonded through their corners. Alumina, by re-ordering bonds and creating Al–O–Al bridges, works as a glass former increasing the glass viscosity. Rare earth oxides, on the other hand, modify the glass structure by supplying oxygen ions and by increasing the O:Si ratio, leading to lower glass viscosity [6,7].

Although compositions in the system SiO<sub>2</sub>–Al<sub>2</sub>O<sub>3</sub>–

RE<sub>2</sub>O<sub>3</sub> are largely applied as sintering additives for covalent ceramics, phase diagrams of these systems have been poorly studied and information is very limited. It is known that for RE=La the eutectic temperature is of approximately 1200 °C [8], while for any other rare earth the eutectic temperature ranges from 1300 to 1400 °C [8]. Some compositions in these rare earth systems can be solidified without crystallization [9]. These compositions lie within the glass-forming region of the phase diagram, typically within the SiO<sub>2</sub>-rich region. The glass-forming region shrinks toward 60%SiO<sub>2</sub>–20%Al<sub>2</sub>O<sub>3</sub>–20%RE<sub>2</sub>O<sub>3</sub> compositions as the rare earth ionic radius decrease [10].

The aim of this work is to investigate silicon carbide interaction with rare earth silicate glasses (RE=Y, La, Nd and Dy).

## 2. Experimental procedure

The starting raw materials were alumina (Alcoa, A16-SG), silica (Fluka) and rare earth oxides (Y<sub>2</sub>O<sub>3</sub>, La<sub>2</sub>O<sub>3</sub>, Nd<sub>2</sub>O<sub>3</sub> and Dy<sub>2</sub>O<sub>3</sub>, Sigma Aldrich). The rare earth oxides were chosen with the aim to provide a spectrum of the entire rare earth family (see Table 1).

The powders were characterized for particle size distribution using the sedimentation method, for phase composition by X-ray diffraction and microstructure by scanning electron microscopy (SEM).

\*Corresponding author.

E-mail address: [jmarchi@net.ipen.br](mailto:jmarchi@net.ipen.br) (J. Marchi).

Table 1  
Properties of rare earth elements/oxides

Element	Z (u.m.a)	A (u.m.a)	Atomic radii (Å)	Ionic radii RE <sup>+3</sup> (Å)	Molecular weight	Density RE <sub>2</sub> O <sub>3</sub> (g/cm <sup>3</sup> )	Electronic configuration
Y	39	88.9	1.78	0.88	225.8	5.01	[Kr]4d <sup>1</sup> 5s <sup>2</sup>
La	57	139.9	1.88	1.040	325.8	6.51	[Xe]5d <sup>1</sup> 6s <sup>2</sup>
Nd	60	144.2	1.82	0.995	336.5	7.24	[Xe]4f <sup>4</sup> 6s <sup>2</sup>
Dy	66	162.5	1.77	0.908	373.0	7.81	[Xe]4f <sup>10</sup> 6s <sup>2</sup>

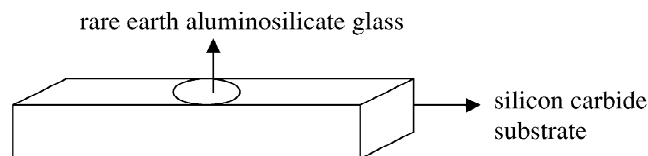


Fig. 1. Schematic representation of glass–SiC system.

Rare earth silicate glasses were prepared within 60%SiO<sub>2</sub>–20%Al<sub>2</sub>O<sub>3</sub>–20%RE<sub>2</sub>O<sub>3</sub> compositions in mol%, hereafter labeled as 6S2A2RE (RE=Y, La, Nd, Dy). The powder mixtures were molten in a platinum crucible at 1500 °C for 1 h and then quickly poured on stainless plates to solidify. The density of glasses was measured by Archimedes method.

Silicon carbide specimens were obtained by cold isostatic pressing of β-SiC powder (H.C. Starck BF-17). The green density reached approx. 55% of the theoretical density.

The glasses prepared were placed on the top of SiC compacts to observe the interaction during thermal treatment. Glass–SiC pairs were annealed in graphite resistance furnace at 1500 °C for 1 h, under argon atmosphere. The glass–SiC couples are hereafter labeled as Y, L, N and D, according to the RE element used in glass composition. The glass–SiC system is schematically shown in Fig. 1. After heat treatment, cross-sections of the specimens were observed on scanning electron microscope.

The concentration profile of rare earth elements through silicon carbide bodies was analyzed by energy dispersive spectroscopy (EDS) to estimate the depth of glass infiltration. The analysis was carried out on selected areas, the

coordinate centers of such areas used to plot the profiles. The relative concentration of rare earth elements was calculated over the total cations amount (Si, Al and RE).

The same glasses were used to sinter silicon carbide ceramics. Specimens containing 90 vol.% silicon carbide and 10 vol.% 6S2A2RE powder mixture were mixed, cold isostatic pressed and sintered at 1950 °C for 1 h, under continuous argon flow.

### 3. Results and discussion

The measured density of rare earth glasses was 3.48, 3.84, 3.89 and 4.19 g/cm<sup>3</sup>, respectively for Y, La, Nd and Dy. It was observed that glass density increases as the ionic radius of rare earth decreases due to increase in rare earth atomic weight. White and Day [2] suggested that this behavior could be also related to improvement in the atomic packing.

Fig. 2 presents the X-ray diffraction patterns of as-received raw materials. All materials appear to be completely crystalline, characterized by narrow diffraction peaks.

Particle morphology of 6S2A2RE powder mixtures is shown in Fig. 3. The particle size distributions are indicated in Fig. 4. The particle size data are in good agreement with microscopy observation, showing particles smaller than 5 μm. The 6S2A2Y distribution probably reveals powders in the agglomerated form, as seen by the broader particle size distribution.

The X-ray diffraction pattern of rare earth glasses is

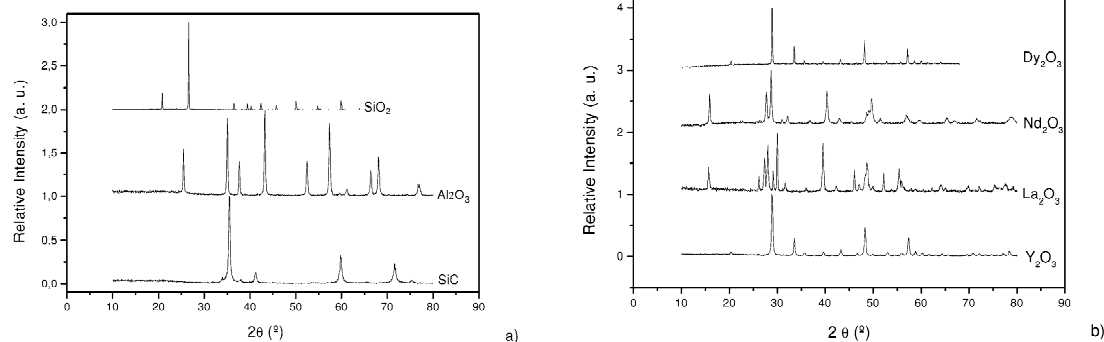


Fig. 2. X-ray diffraction pattern of as-received powders: (a) silica, alumina and silicon carbide; and (b) rare earth oxides (yttria, lanthania, neodymia and dysprosia).

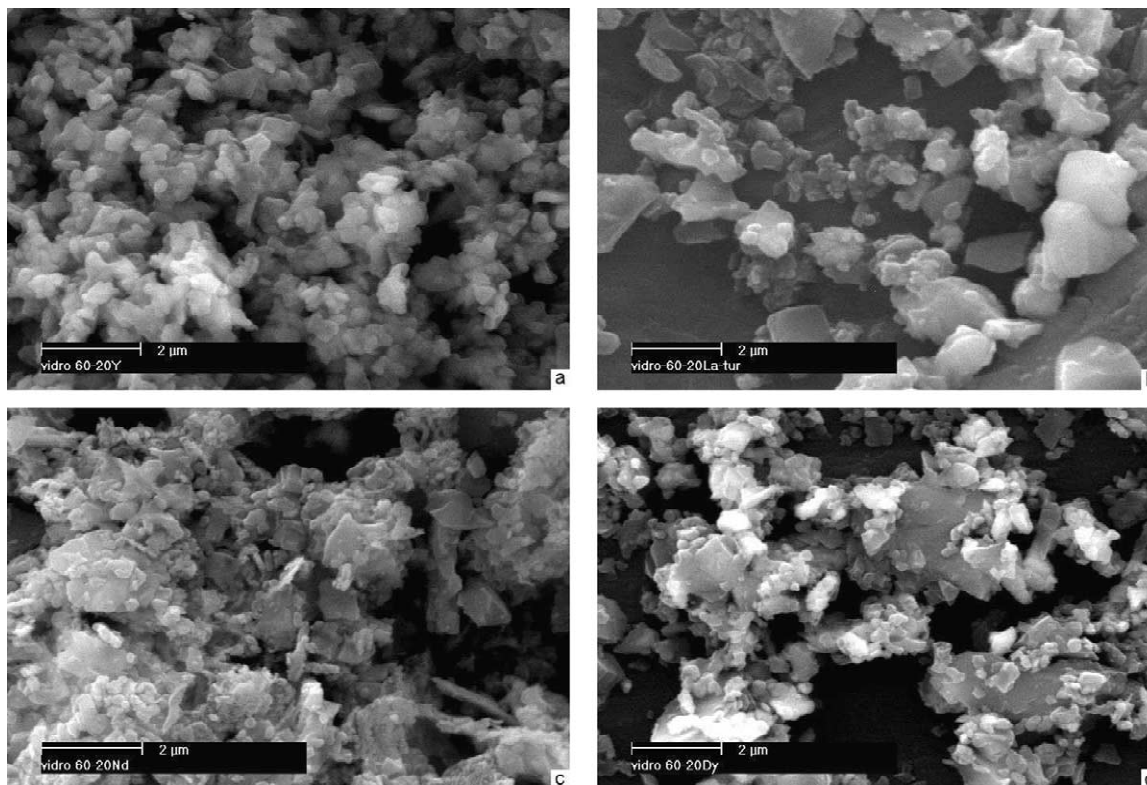


Fig. 3. Scanning electron micrographs of  $60\text{SiO}_2-20\text{Al}_2\text{O}_3-20\text{RE}_2\text{O}_3$  compositions: (a)  $\text{Y}_2\text{O}_3$ ; (b)  $\text{La}_2\text{O}_3$ ; (c)  $\text{Nd}_2\text{O}_3$ ; and (d)  $\text{Dy}_2\text{O}_3$ .

presented in Fig. 5. All glasses display an amorphous phase pattern. This indicates that the temperature/time conditions used herein were sufficient to produce rare earth silicate glasses. Slight differences in particle size distribution of various powders did not influence homogeneity in the mixtures, leading to compositions that, after melt, were completely amorphous.

After annealing, glass–SiC pairs were cut to examine the interaction zone. For all systems, glass completely

infiltrated the silicon carbide body, the interface having a convex shape. As SiC sintering temperature ( $1950^\circ\text{C}$ ) is higher than the annealing temperature (approx.  $1500^\circ\text{C}$ ), densification of the matrix was in general not present. However, the interaction zone appears to be stronger than the silicon carbide body.

Fig. 6 depicts the scanning electron micrographs of glass–SiC cross-sections showing the interaction zone. The

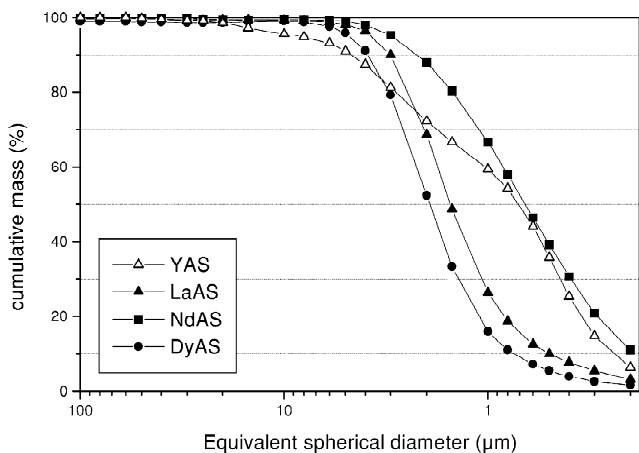


Fig. 4. Particle size distribution of  $60\text{SiO}_2-20\text{Al}_2\text{O}_3-20\text{RE}_2\text{O}_3$  compositions.

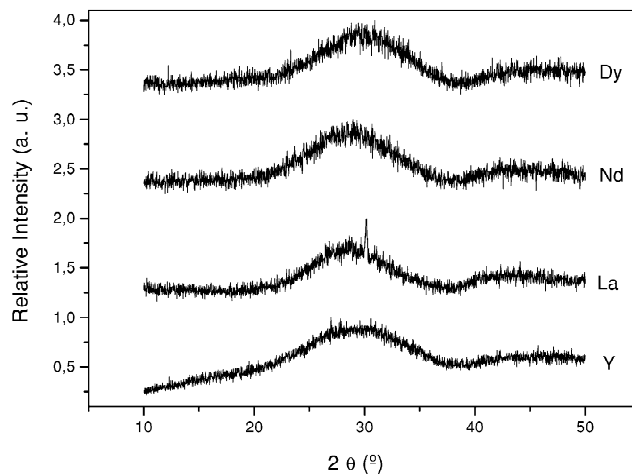


Fig. 5. X-ray diffraction pattern of rare earth silicate glasses obtained after melting at  $1500^\circ\text{C}/1\text{ h}$ .

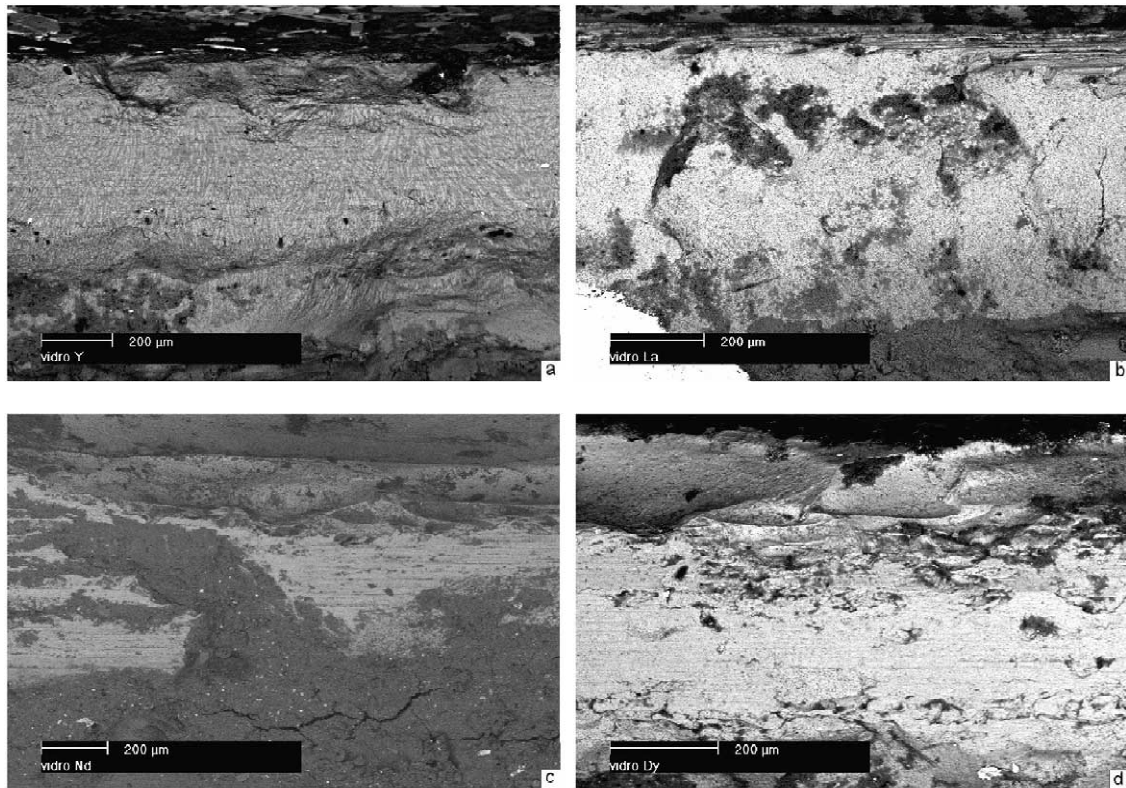


Fig. 6. Scanning electron micrographs of rare earth glass–SiC interaction zone: (a)  $\text{Y}_2\text{O}_3$ ; (b)  $\text{La}_2\text{O}_3$ ; (c)  $\text{Nd}_2\text{O}_3$ ; and (d)  $\text{Dy}_2\text{O}_3$ .

regions that contain rare earth elements appear in light gray. Rare earth concentration distribution appears to be homogeneous for Y and D couples and very discontinuous for L and N couples. The interaction zone width is 500, 1100, 400 and 800  $\mu\text{m}$  for Y, L, N and D couples, respectively, as seen by scanning electron micrographs.

Fig. 7 represents the concentration profile of rare earth elements across the interaction zone. The L couple exhibits the highest degree of rare earth infiltration and a different behavior profile, showing higher concentration at the bottom of the interaction zone. This behavior is due to the low viscosity of  $\text{LaSiAlO}$  glass, which enables easier flow through SiC compounds.

On the other hand, the infiltration profile of N–SiC couple shows that  $\text{NdSiAlO}$  glasses have the lowest slippage behavior. A weak interaction with the silicon carbide can be noticed. Hence, in this case, the profile is affected by the low wettability and high viscosity of  $\text{NdSiAlO}$  glasses.

On the following studies of sintering silicon carbide with additives at 1950  $^\circ\text{C}/1$  h, it was observed that all samples had a great weight loss of about 15%. The final density values were 82.9, 69.9, 66.8 and 81.0% of the theoretical density, respectively for Y, La, Nd and Dy as rare earth additives. SiC containing Y and Dy as additives exhibited higher final densities due to good wetting behavior, even at low temperatures.

#### 4. Conclusions

The results indicate that even though  $\text{SiO}_2\text{--Al}_2\text{O}_3\text{--RE}_2\text{O}_3$  systems with different substitutions ( $\text{RE}=\text{Y}$ , Nd and Dy) have similar eutectic temperature, the interactive behavior between rare earth silicate glass and silicon carbide depends on the type of rare earth cation.  $\text{SiO}_2\text{--Al}_2\text{O}_3\text{--La}_2\text{O}_3$ , due to the lowest eutectic temperature, has the highest wettability and infiltration behavior.

The experiments presented herein are efficient in indicating the best additives for liquid-phase sintering of silicon carbide based ceramics. Y and Dy show high wettability on SiC. For these rare earth oxides, the use of an intermediate dwell time (at 1500  $^\circ\text{C}$ ) on sintering is suggested. This temperature can be successfully employed to improve the distribution of  $\text{SiO}_2\text{--Al}_2\text{O}_3\text{--RE}_2\text{O}_3$  additives in silicon carbide matrix, resulting in high density ceramics.

#### Acknowledgements

The authors would like to thank CNPq and PRONEX/FINEP for financial support, and Laboratório de Materiais Vítreos, DEMA, UFSCar. The authors would also like to thank Ms Daniel S. Moraes for discussions and Dr Pilar S. Sepulveda for help with English.

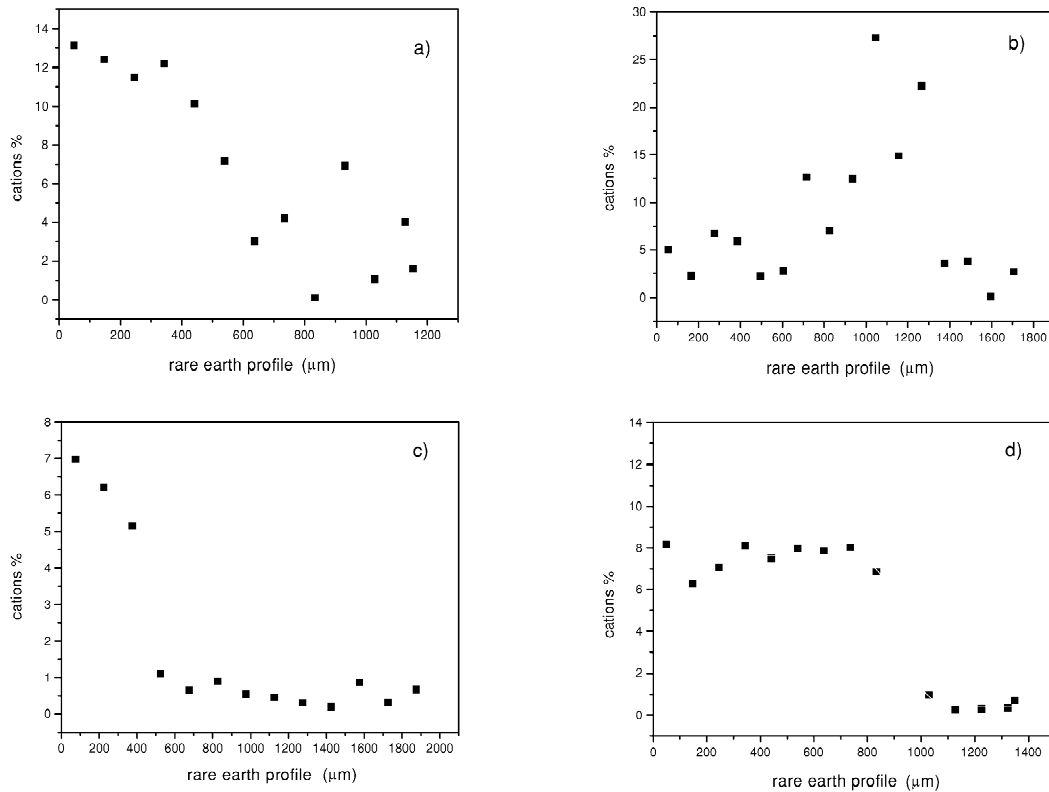


Fig. 7. Concentration profile along rare earth glass-SiC interaction zone: (a)  $Y_2O_3$ ; (b)  $La_2O_3$ ; (c)  $Nd_2O_3$ ; and (d)  $Dy_2O_3$ .

## References

- [1] A.G. Clare, Key Engineering Materials, in: J.E. Shelby et al. (Eds.), Rare Elements in Glasses, Vols. 94–95, Trans Tech Publications, Switzerland, 1994, pp. 161–180.
- [2] J.E. White, D.E. Day, Key Engineering Materials, in: J.E. Shelby et al. (Eds.), Rare Elements in Glasses, Vols. 94–95, Trans Tech Publications, Switzerland, 1994, pp. 181–208.
- [3] M. Keppeler, H.G. Reichert, J.M. Broadley, G. Thurn, I. Wiedmann, J. Euro. Ceram. Soc. 18 (1998) 521–526.
- [4] F.K. Van Dijen, E. Mayer, J. Euro. Ceram. Soc. 16 (1996) 413–420.
- [5] V.A. Izhevskiy, La.A. Genova, A.H.A. Bressiani, J.C. Bressiani, Mater. Res. 4 (2000) 131–138.
- [6] Y.M. Chiang, D.P. Birnie III, W.D. Kingery, Physical Ceramics, Wiley, EUA, 1997.
- [7] J. Zarzyck, Glasses and the Vitreous State, Cambridge University Press, Cambridge, 1991.
- [8] U. Jolitsch, H.J. Seifert, F. Aldinger, J. Phase Equil. 19 (1998) 426–433.
- [9] I.H. Arita, D.S. Wilkinson, G.R. Purdy, J. Am. Ceram. Soc. 75 (1992) 3315–3320.
- [10] J.E. Shelby, Key Engineering Materials, in: J.E. Shelby et al. (Eds.), Rare Elements in Glasses, Vols. 94–95, Trans Tech Publications, Switzerland, 1994, pp. 1–42.